5-7-2010

A Reactive Molecular Dynamics Simulation Of The Silica-Water Interface

Joseph C. Fogarty
University of South Florida

Hasan Metin Aktulga
Purdue University - Main Campus, hmaktulga@lbl.gov

Ananth Y. Grama
Purdue University, ayg@cs.purdue.edu

Adri C. T. Van Duin
Pennsylvania State University

Sagar A. Pandit
University of South Florida

A reactive molecular dynamics simulation of the silica-water interface

Joseph C. Fogarty,[1,a)] Hasan Metin Aktulga,[2] Ananth Y. Grama,[2] Adri C. T. van Duin,[3] and Sagar A. Pandit[1,b)]
[1]*Department of Physics, University of South Florida, Tampa, Florida 33620-9951, USA*
[2]*Department of Computer Science, Purdue University, West Lafayette, Indiana 47907-2107, USA*
[3]*Department of Mechanical and Nuclear Engineering, Pennsylvania State University, University Park, Pennsylvania 16802-1414, USA*

(Received 8 January 2010; accepted 31 March 2010; published online 4 May 2010)

We report our study of a silica-water interface using reactive molecular dynamics. This first-of-its-kind simulation achieves length and time scales required to investigate the detailed chemistry of the system. Our molecular dynamics approach is based on the ReaxFF force field of van Duin *et al.* [J. Phys. Chem. A **107**, 3803 (2003)]. The specific ReaxFF implementation (SERIALREAX) and force fields are first validated on structural properties of pure silica and water systems. Chemical reactions between reactive water and dangling bonds on a freshly cut silica surface are analyzed by studying changing chemical composition at the interface. In our simulations, reactions involving silanol groups reach chemical equilibrium in ~250 ps. It is observed that water molecules penetrate a silica film through a proton-transfer process we call "hydrogen hopping," which is similar to the Grotthuss mechanism. In this process, hydrogen atoms pass through the film by associating and dissociating with oxygen atoms within bulk silica, as opposed to diffusion of intact water molecules. The effective diffusion constant for this process, taken to be that of hydrogen atoms within silica, is calculated to be 1.68×10^{-6} cm^2/s. Polarization of water molecules in proximity of the silica surface is also observed. The subsequent alignment of dipoles leads to an electric potential difference of ~10.5 V between the silica slab and water. © *2010 American Institute of Physics*. [doi:10.1063/1.3407433]

I. INTRODUCTION

Amorphous silica (a-SiO_2), its surface properties, and hydrolysis have been topics of research in diverse application domains ranging from geosciences to nanoelectronics. The high dielectric constant and selectivity for chemical modification make silica among the most widely used substrates in the design of nanoelectronic devices. Recent advances in molecular biology have demonstrated its use in devices capable of performing *in vivo* screening of biomolecules and biomolecular processes, along with other applications in biotechnology that rely on surface modification of silica. Silica can serve as a substrate for biosensors, electronic components, and enzymes.[1,2] Since these devices are often required to function in inhospitable aqueous cellular environments, a detailed understanding of their interactions with water is crucial.

Experimental methods such as infrared spectroscopy,[3–5] x-ray crystallography,[6,7] nuclear magnetic resonance,[8] and electron microscopy do not sufficiently describe the processes by which silica is corroded by water at an atomic scale.[9] Molecular dynamics (MD) techniques, due to their ability to probe nanoscale spatiotemporal processes, can provide valuable insights into this problem. Conventional classical MD has the ability to simulate bulk properties of a-SiO_2.[10–13] It lacks, however, the ability to model chemical reactions, specifically the dissociation of water and the resulting recombination of O and OH units with the silica surface. Consequently, while conventional MD simulations can yield reliable data on bulk silica, they do not sufficiently describe interfacial properties of interest.[10] In a significant effort, Garofalini *et al.* simulated water-silica interaction using MD with a dissociative water model.[14] In this paper, we put forth several new observations using a more general reactive potential that incorporates variable charges as well as confirm a number of observations of Garofalini *et al.* A reactive potential allows changes in bond order, which coincide with changes in electron densities, thereby implying modification of partial charges. The current work also extends the scale of reactive simulations.

Quantum mechanical *ab initio* methods have been used to simulate chemical reactions at the silica-water interface.[10,15] These simulations are typically limited to subnanometer length and picosecond time scales. For this reason, *ab initio* approaches are unable to simultaneously describe bulk systems and interfaces. Due to limitations on scalability, surface characteristics of silica in *ab initio* simulations are artificially constructed, as opposed to being derived from an annealing process.[16] These *ab initio* simulations generally also ignore the interaction of the interfacial section with the silica bulk. Attempts have been made to bridge this gap using hybrid simulation techniques, whereby the surface sites are simulated using quantum calculations and bulk sections are simulated using classical MD.[17] This approach has potential drawbacks due to the interface between the *ab initio* and MD regions of the system. Classical

a)Electronic mail: jcfogart@mail.usf.edu.
b)Electronic mail: pandit@cas.usf.edu.

force fields must be tuned not only to fit experimental results but also to interface with the *ab initio* calculations. Inconsistencies between MD force fields and quantum calculations can result in unwanted changes in the structure of the system.[15]

In this work, we use a novel MD force field, ReaxFF, developed by van Duin *et al.*[18] This method relies on the development of empirical force fields that mimic the quantum mechanical variation of bond order. ReaxFF replaces the harmonic bonds of conventional MD with bond orders and energies that depend on interatomic distances. Valencies, explicitly satisfied in MD simulation, necessitate many-body calculations in ReaxFF. The approach allows bond order and all bonded interactions to decay smoothly to zero, allowing chemical reactions within a MD framework. Consequently, ReaxFF can overcome many of the limitations inherent to nonreactive MD while retaining, in large part, the desirable scalability. The applicability of ReaxFF to large scale silica systems has been questioned on the basis of its computational cost.[19] State-of-the-art implementations (SERIALREAX), however, have demonstrated excellent computational efficiencies, thereby greatly alleviating scalability concerns.

In this paper, we present the results of a reactive MD simulation of a water-silica system. We show that ReaxFF is able to reproduce bulk properties of silica and water to a high degree of accuracy, silica surface properties in agreement with that of *ab initio* calculations, and predict chemical reactions at the interface. To the best of our knowledge, no other computational approach satisfactorily addresses all three aspects of this problem simultaneously.

II. METHODS

All of the MD simulations in the paper are performed using SERIALREAX molecular simulation software version 2.0.0.[20] ReaxFF differs from a classical MD approach in several fundamental ways.

- Although no statistical mechanical approach would ever formally assume distinguishability, indistinguishability is completely required in the analysis of reactive simulations. ReaxFF allows atoms to move from one chemical species to another. Consequently, interpretation of ReaxFF data must assume the indistinguishability of particles, inherent to any quantum mechanical system, even though the assumption is not explicit in the simulation technique itself. Specifically, for our system, oxygen atoms may transition between water and silica and hence cannot be labeled as members of specific chemical species.
- The bond order term and its corrections force the ReaxFF potential to be inherently many-body. Consequently, all force field terms dependent on bond order become many-body interactions. This makes the calculation of a reactive potential more computationally expensive than a classical MD approach.
- The SERIALREAX model incorporates a charge equilibration technique (QEq) introduced by Rappé and Goddard.[21] This approach seeks to minimize electrostatic energy by assigning partial charges based on ionization potential, electron affinities, and atomic radii. The total electrostatic energy and atomic chemical potential are given by

$$E_Q(Q_1 \ldots Q_N) = \sum_A (E_{A0} + \chi_A^0 Q_A) + 1/2 \sum_{A,B} Q_A Q_B J_{AB}, \tag{1}$$

$$\chi_A(Q_1 \ldots Q_N) = \chi_A^0 + J_{AA}^0 Q_A + \sum_{B \neq A} J_{AB} Q_B. \tag{2}$$

  Total energy is then minimized with the constraints that total charge remains constant and that all atomic chemical potentials remain equal. Implementation of QEq requires the solution of a large system of linear equations with constraints. In SERIALREAX, this large system of equations is solved at every step using an efficient preconditioned linear solver [GMRES (Ref. 22)].
- Reordering of chemical species within ReaxFF requires dynamic neighbor lists, even for bonded interactions, such as bond, angle, and torsion. This requires careful design and orchestration of dynamic data structures within SERIALREAX to minimize computational overhead with regard to classical MD.

These differences add significant complexity to ReaxFF implementations when compared to a classical MD approach. SERIALREAX relies on a range of sophisticated algorithms, data structures, and numerical techniques to minimize the cost of these computations. As a result, ReaxFF retains much of desirable scalability of classical MD but adds considerable simulation power.

A. System preparation

1. Preparation of a-SiO_2 system

Since ReaxFF updates bond order and bond order dependent quantities at every time-step, it requires a smaller time-step than conventional MD approaches.[23] Chemical reactions occur over subpicosecond time scales. Thus, all simulations were performed with a 0.5 fs time-step. All simulations, unless otherwise noted, were performed at a temperature of 300 K. A Nosé–Hoover thermostat was used in each case to couple the system to a heat reservoir.[24] Whenever a constant pressure and temperature (*NPT*) ensemble was utilized, a Berendsen barostat and thermostat were used to couple to a bath.[25,26] A Berendsen barostat was preferred over a Parrinello–Rahman barostat to avoid large pressure fluctuations, which can lead to unrealistic chemical reactions.

The amorphous silica system was constructed by initially placing 2000 silica (SiO_2) molecules randomly in a $67.4 \times 67.4 \times 20.0$ $Å^3$ box, resulting in a silica system with an initial density of 2.2 g/cm^3. To eliminate atomic overlaps and bad contacts, the system was energy-minimized in a microcanonical (*NVE*) ensemble for 50 ps. The bulk and surface properties of a silica system are highly dependent on the annealing procedure.[27] Simulation of an amorphous silica slab with the correct structural properties requires very high temperature annealing.[28] Hence, the system was annealed

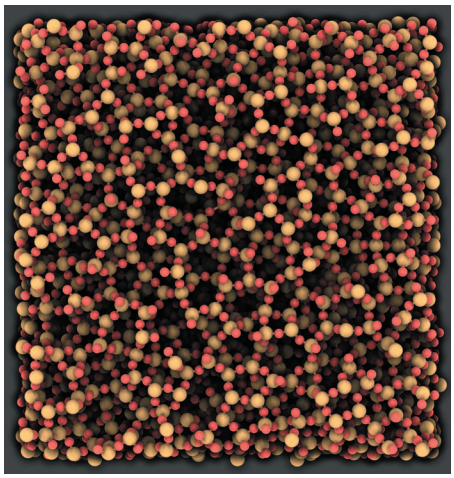

FIG. 1. Surface of annealed silica. Undercoordinated silicon atoms are bound to only three oxygen atoms. Undercoordinated oxygen atoms are bound to only one silicon atom. [Image generated with QUTEMOL (Ref. 29).]

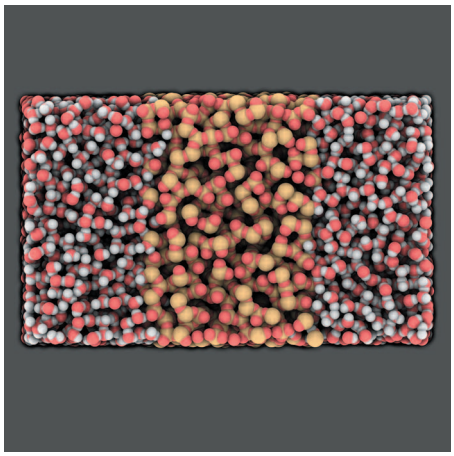

FIG. 2. System snapshot: z-axis shown as horizontal. Oxygen (red), hydrogen (white), and silicon (yellow) atoms shown. [Image generated with QUTEMOL (Ref. 29).]

twice from 4000 to 300 K. In the first annealing simulation, the system was heated to 4000 K and gradually cooled to 300 K with steps of 100 K per 4 ps using *NVT* ensemble. The system was again heated to 4000 K using an *NPT* ensemble for ~75 ps until the system completely melted and formed a uniform block with dimensions of $52.110 \times 50.174 \times 36.477$ Å^3. The system was again cooled, still in an *NPT* ensemble, to 300 K in steps of 100 K per 4 ps. All *NPT* simulations were conducted at a constant pressure of 1 atm. The final annealed system was used to perform a continuous simulation of 185 ps for validation of silica properties. The same system was also used for the silica-water interface simulation. Figure 1 shows a freshly cut surface of annealed silica.

2. Preparation of pure water system

The water system was prepared by filling a box of size $51.800 \times 49.900 \times 23.600$ Å^3 (chosen to fit the silica system) with 2025 water molecules. This resulted in a density of 0.99 g/cm^3. Water molecules were added with random alignment and location (avoiding overlap). The system was then thermalized under an *NVT* ensemble for 664 ps. A *NPT* ensemble was not used due to the need to fit the water box to the silica slab. Although semi-isotropic pressure coupling would have allowed for a *NPT* ensemble, it was not available in the SERIALREAX version used in this work. This system was used both for the interface simulation and the validation of water properties. Position, bond, and angle data were output every 500 steps for water verification analysis.

3. Preparation of silica-water interface

The water and silica systems described above were combined by positioning copies of the water system normal to the z-axis and adjacent to the silica system, resulting in total system dimensions of $52.110 \times 50.174 \times 83.700$ Å^3. The system was then simulated under the *NVT* ensemble. *NVT* was used instead of *NPT* because the difference in compressibility between a-SiO_2 and water would cause unrealistic pressure effects. After 70 ps, the simulation was then restarted with velocities randomly generated to fit the set temperature. Velocities were reset in order to remove any artifacts from the system construction. The simulation was then run for a total of 580 ps. The system maintained thermal equilibrium with the heat bath for the final 150 ps. Therefore, these steps were used for structural and electrostatic analysis. As the reactions between water and the silica slab took place in the first 150 ps of the run, chemical analysis was performed on these initial steps. For the final 370 ps of simulation, position, velocity, bond, and angle data were written every 250 steps. Figure 2 shows a snapshot of the simulated system.

B. Force field parameters

To obtain a ReaxFF description capable of describing the reactions at the SiO_2/water interface we modified the ReaxFF Si/O/H parameters described by van Duin *et al.*[30] While these parameters could describe Si/SiO_2 interfaces, they were solely based on quantum mechanical (QM) data describing radical reactions and were thus unable to describe the energetics related to proton-transfer reactions at the water/silica interface. To extend ReaxFFSiO(2003) to these reactions, we first replaced the O/H parameters with a set of ReaxFF O/H parameters fitted against water-clusters and proton-transfer reactions in $H_3O^+[H_2O]n$ and $OH^-[H_2O]_n$ systems.[31] Keeping the O/H parameters fixed, we subsequently refitted the Si/O, Si/Si, and Si/H bond and angle parameters against the QM-based training set data used to fit ReaxFFSiO(2003). These data included bond dissociation curves for all Si/O/H bond combinations, angle distortion energies for all Si/O/H angle combinations, and equations of state for bulk-Si and bulk-SiO_2-data. To augment this training set for water/silica cases, we added two additional sets of QM-based data (at the DFT/B3LYP/6-311G**++ level of theory) to the training set. These sets described (i) the binding and dissociation of a single water molecule from a $Si(OH)_4$ molecules and (ii) reaction energies for the $Si(OH)_4$ polymerization.[32] Figure 3 and Table I compare the ReaxFF

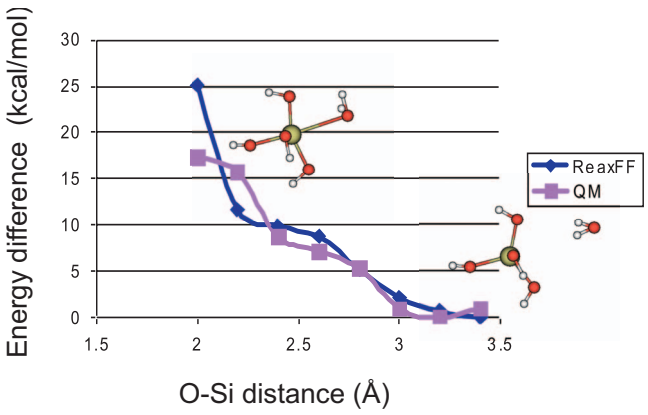

FIG. 3. Reax force field validation.

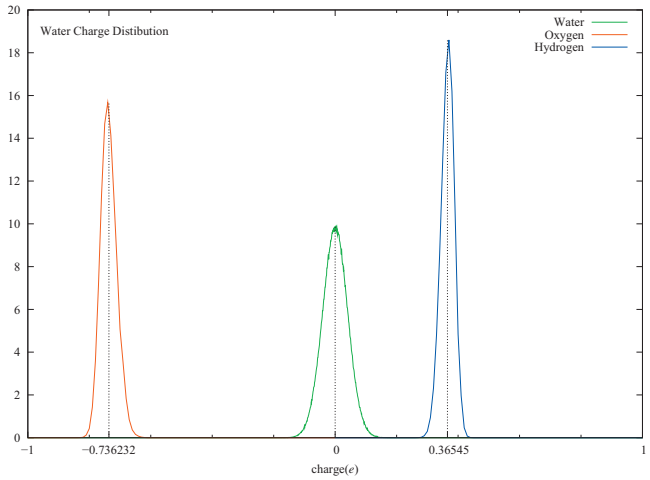

FIG. 4. Water charge distribution. Water molecule charge is distributed about neutral, with oxygen and hydrogen charges distributed about $-0.736e$ and $0.365e$, respectively.

results to the QM-data for these two cases, indicating that ReaxFF can successfully describe both the nonreactive interaction of a water molecule with a hydroxylated silica surface and the reaction energies associated with silica formation.

III. RESULTS

A. Validation of models

1. Water

Validation of the water model involves computation of the average structural properties of a single water molecule and the static and dynamic properties of bulk water. Table II shows a comparison of water properties computed using our model with those of *ab initio* simulations and experiments. In spite of several approximating assumptions, our model reproduces several key properties of water. The oxygen-hydrogen bond length (d_{OH}) in the first line is the average distance between oxygen and hydrogen atoms that share a bond order $\geq \frac{1}{2}$. We note that the model reproduces experimental data for bond length and angle within the standard deviations. The partial charges (lines 3 and 4) on oxygen and hydrogen atoms (q_O and q_H) result from the QEq process. These charges (please see Fig. 4) are lower than the popular fixed charge water models, such as simple point charge (SPC) and extended simple point charge (SPC/E). Lower charges are expected since fixed charge models rely on a mean field approximation of large partial charges to reproduce bulk properties of liquid water.[42]

Coordinate independence of the dipole moment vector requires molecular charge neutrality. While the QEq method implemented in SERIALREAX software imposes a constant charge constraint on the entire system, it does not require molecules to be charge neutral. Hence, computation of the electrical dipole moment of water in ReaxFF is nontrivial. To enforce neutrality, half of the oxygen charge was assigned to each hydrogen atom, ignoring the hydrogen charge computed by QEq. Figure 4 shows the distribution of charge on water molecules. The standard deviation of water charge about a neutral molecule is $4.1 \times 10^{-2}e$, which indicates that a substantial number of water molecules are not neutral. However, the distribution suggests that the molecular charge constraint is only marginally violated by the QEq procedure. Consequently, approximations involved in computation of dipole moment introduce negligible error. The average dipole moment in a water cluster has been established by both experiment[37] and theory[43] to be larger than that of an isolated molecule. The dipole moment reported for *ab initio* simulation is for an isolated molecule, while the value presented here is for bulk water.

TABLE I. Water data.

Reaction	ReaxFF	QM[a]
$Si(OH)_4+Si(OH)_3O^- \rightarrow (OH)_3Si-O-Si(OH)_2O^-$ $+H_2O$(dimer anion)$+H_2O$	−23.0	−20.8
$(OH)_3Si-O-Si(OH)_2O^-+Si(OH)_4$ $\rightarrow (OH)_3Si-O-Si(OH)_2-O-Si(OH)_2O^-+H_2O$ (trimer anion$+H_2O$)	−18.9	−14.3
$(OH)_3Si-O-Si(OH)_2-O-Si(OH)_2O^-+Si(OH)_4$ $\rightarrow$branched quadrimer anion$+H_2O$	−24.0	−28.9

[a]Reference 32.

The structure factor describes the scattering interaction between incident particles and the form of the scattering medium. Structure factor is not dependent on the nature of the interaction itself but rather on the geometry of the system alone. A Fourier transform on the density function produces the structure factor.[44] Since the radial distribution function (RDF) is dependent on the density function, it can be used to predict the results of scattering experiments. The RDF between two atomic species is defined as

$$g(r) = \frac{N(r)}{4\pi r^2 \rho \delta r}, \tag{3}$$

where $N(r)$ is the number of type 2 atoms in the shell between r and $r+\delta r$ around the type 1 atoms and ρ is the number density of type 2 atoms, taken as the ratio of the number of atoms to the volume of the simulation cell. Table II (rows 8 and 9) lists the properties derived from O–O RDF. The RDF for water is presented in Fig. 5.

The diffusion coefficient (row 10 of Table II) of oxygen in water is representative of its translational mobility. It can be calculated from the long time behavior of the mean square displacement (MSD) of the atom using the Einstein relation

TABLE II. Water data. Reax results compared with *ab initio*, SPC/E, and experimental. Water bond length is given as d_{OH}. RDF minimum and maximum values are local min and max. Diffusion is atomic self-diffusion.

Property	ReaxFF	SPC/E[a]	*Ab initio* BLYP[b]	Experimental
d_{OH} (Å)	0.98 ± 0.04	1.000	0.973	0.957[c]
HOH angle (°)	104 ± 4	109.47	104.4	104.5[d]
q_O (e)	−0.73 ± 0.03	−0.8476	⋯	⋯
q_H (e)	0.36 ± 0.03	0.4238	⋯	⋯
μ (D)	2.1 ± 0.2	2.35	1.81	2.9[e]
OO distance (Å)	2.88 ± 0.2	⋯	2.95	2.98[f]
OHO angle (°)	168 ± 6	⋯	173	174[g]
OO RDF first max. (Å)	2.77	⋯	2.80	2.82[h]
OO RDF first min. (Å)	3.35	⋯	3.35	3.51[h]
D_O (Å^2/ps)	0.29	0.249	0.13	0.24[i]
D_H (Å^2/ps)	0.29	⋯	⋯	⋯

[a]Reference 33.
[b]Reference 34.
[c]Reference 35.
[d]Reference 36.
[e]Reference 37.
[f]Reference 38.
[g]Reference 39.
[h]Reference 40.
[i]Reference 41.

$$D = \lim_{t\to\infty} \frac{\langle |\vec{r}(t) - \vec{r}(t_0)|^2 \rangle}{6(t - t_0)}, \tag{4}$$

where $\vec{r}$ is the position of the atom. The MSD of each atom was calculated over 166 ps intervals in the 664 ps production run. A least-squares straight-line fit of the trajectory averaged MSD was then performed over the subinterval from 40 to 166 ps within the 166 ps interval. Figure 6 shows the MSD of water oxygen and hydrogen as a function of time. The diffusion coefficients of these two atomic species do not show significant difference. This indicates that water diffuses in bulk water mostly as entire molecules without dissociation.

2. Silica

The validation of the amorphous silica model involves computation of structural properties including mass density, bond lengths, bond angles, and RDFs. Table III reports these properties for the simulated model and a comparison with *ab initio* and experimental values.

Though the reported density for silica in ReaxFF is lower than that from classical MD and experiments, the specifics of the annealing process have an effect on the structural properties of the final system. The silicon-oxygen bond length (d_{SiO}), calculated as the average distance between bonded silicon and oxygen atoms, is in agreement with both experiment and MD. Angles within a tetrahedra (O–Si–O angles) and between two tetrahedra (Si–O–Si angles) are given, along with full width at half maximum (in parentheses). There is a wide range of Si–O–Si angles from 120 to 180, which is a fundamental difference between crystalline silica and a-SiO_2.[6]

Important aspects of the RDF for a-SiO_2 are also reported in Table III. The maximum values in the RDF (RDF max.) show the most likely distance between the two atomic species in a specific coordination shell. A minimum value indicates the radius of the shell. The average coordination numbers for silicon and oxygen (Si and O coordination, respectively), which are determined by counting the number of atoms within the first coordination shell, reflect the high level of coordination in bulk silica. The RDFs are presented in Fig. 7.

B. Silica-water interface

ReaxFF allows the application of a broad range of analytical techniques. This approach yields information about the change in concentration of chemical species, which otherwise would not be available to MD simulation. ReaxFF is capable of probing length and time scales that permit utilization of thermodynamic and statistical tools. As a result, the silica-water interface described produces a large amount of information. The data can be interpreted to determine the structural properties of the system, i.e., system geometry, bond characteristics, and molecular orientations. The scope of this analysis cannot be reached by *ab initio* calculations. Unlike other classical MD approaches, ReaxFF generates data regarding the chemical composition of the system. Starting with pure water and pure silica, we end with a hydroxylated silica surface covered by silanol (Si–OH) groups. The

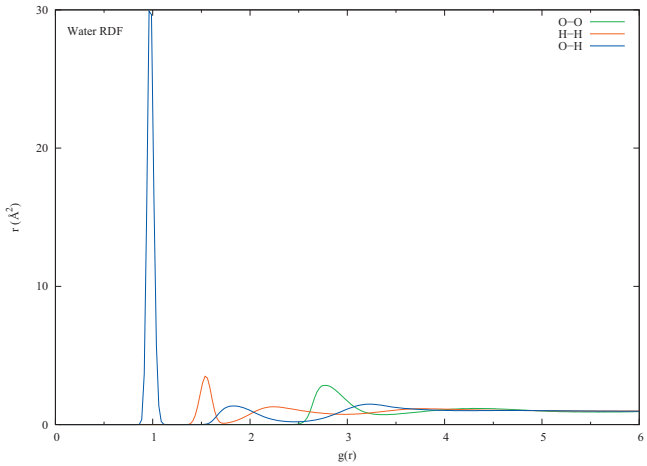

FIG. 5. Water RDF: RDF between oxygen-oxygen (O–O), hydrogen-hydrogen (H–H), and oxygen-hydrogen (O–H) shown for bulk water.

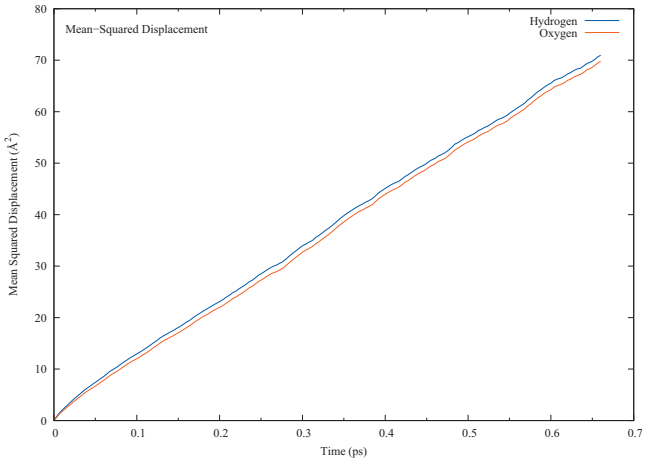

FIG. 6. Water MSD: mean squared displacement shown for oxygen and hydrogen atoms within a pure water system.

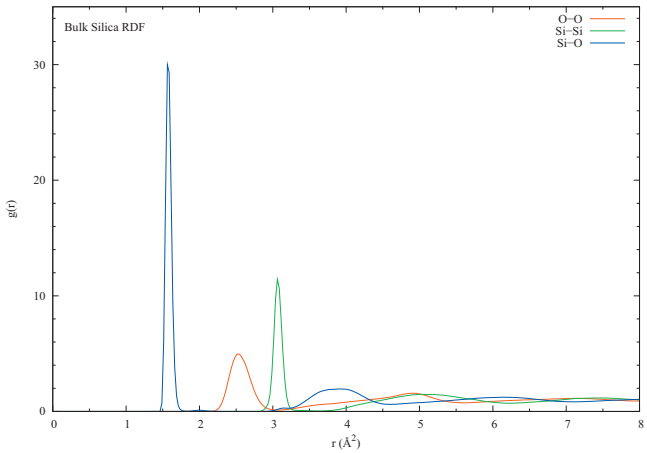

FIG. 7. Silica RDF: RDFs in pure silica shown for oxygen-oxygen (O–O), silicon-silicon (Si–Si), and silicon-oxygen (Si–O).

orientation of the water dipole moment gives rise to electric polarization along silica-water surface. This charge distribution gives rise to a measurable potential difference between the water bulk and the silica bulk. ReaxFF facilitates predictions for new experimental techniques to investigate this.

Since ReaxFF is able to simulate chemical reactions, the approach yields statistically valid samples of reactants produced by the silica-water interface, mostly notably silanol. We are also able to calculate the bond lengths and angles in SiOH units.

1. Structural properties

Figure 8 shows the mass density for the interfacial system as well as its constituent atoms. The system was cut into 0.5 Å slabs along the z-axis, and a mass was calculated for each. The large variations seen in the silica bulk result from the lack of fluidity at room temperature in a-SiO_2, which prevents the averaging out of local density extrema. A peak in the total mass density near the surface results from an increase in the oxygen mass density. This local maximum is a result of the strong alignment of water dipole moment with the silica surface. As is clearly illustrated in Fig. 8, a sharp boundary between water and silica does not exist.

Thus, in order to clearly describe the interfacial area, a Gibbs dividing surface (z_G) was defined on each water-silica interfacial area (Fig. 9). The dividing surface is chosen such that[49]

$$\int_{-\infty}^{z_G} (n(z) - n_1)dz = -\int_{z_G}^{\infty} (n(z) - n_2)dz, \tag{5}$$

where n is the number density of silicon atoms and the bounds at $-\infty$ and ∞ are defined as the points at which n is randomly distributed about n_1 or n_2, respectively. Silicon atoms located outside of these boundaries are defined as being located in the interface, while hydrogen atoms located within these boundaries are defined as being part of the silica bulk. The silica system had a width of 36.5 Å before the addition of water. An identical analysis was performed using hydrogen number density, which yielded results that differed by less than 0.5 Å. The width of bulk silica, defined as the

TABLE III. Silica data. Pure silica in Reax computed with MD and experiment. Silicon oxygen bond is given as d_{SiO}. Max and min RDF values are local min and max values. Coordination is calculated as the average number with the first coordination shell. Full width at half maximum is given in parentheses.

Property	ReaxFF	MD	Experiment
Density (g/cm^3)	2.14	2.23[a]	2.20[b]
d_{SiO} (Å)	1.59 ± 0.07	1.62 ± 0.05[c]	$1.608 \pm .004$ [d]
Si–Si dist. (Å)	3.0 ± 0.2	⋯	⋯
O–O dist. (Å)	2.7 ± 0.3	⋯	2.65[b]
Si–O–Si angle (°)	150 (21.5)	152 (35.7)[e]	144 (38),[b] 153[f]
O–Si–O angle (°)	109.2 (20.9)	108.3 (12.8)[e]	109.4,[f] 109.5[b]
Si–O RDF first max. (Å)	1.56	1.595[e]	1.608,[d] 1.620[b]
Si–O RDF first min.	2.5	⋯	⋯
Si–O RDF second max.	3.90	4.12[e]	4.15[b]
O–O RDF first max.	2.53	2.590[e]	2.626,[d] 2.65[b]
Si–Si RDF first max.	3.06	3.155[e]	3.077, 3.12[b]
Si coordination	3.98	⋯	⋯
O coordination	1.99	⋯	⋯

[a]Reference 45.
[b]Reference 6.
[c]Reference 46.
[d]Reference 47.
[e]Reference 27.
[f]Reference 48.

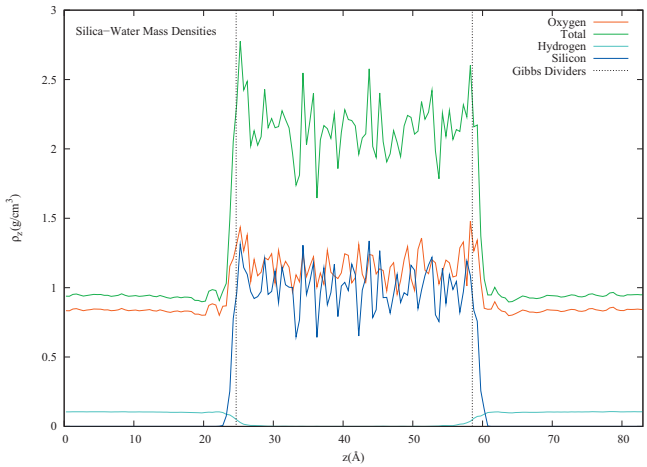

FIG. 8. Mass densities: Mass densities for the interfacial system, illustrating the locations of the Gibbs dividers (dashed). Included is density of oxygen (red), hydrogen (teal), silicon (blue), and the total (green).

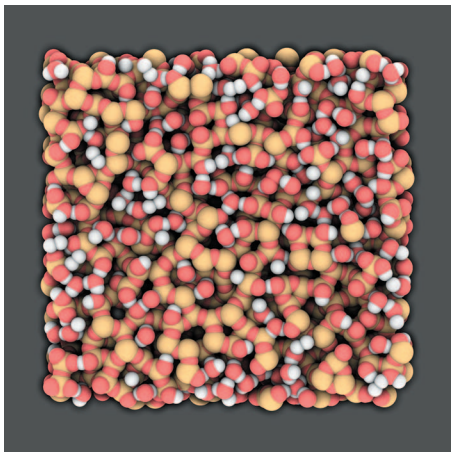

FIG. 9. Silica-water interfacial area. [Image generated with QUTEMOL (Ref. 29).]

distance separating the Gibbs dividers, is 33.9 Å.

In the reaction with water and a freshly cut silica surface, hydrogen penetration into the silica bulk has been observed as evidenced by Fig. 8. Table IV shows atomic diffusion in the silica bulk (within the Gibbs dividers) for hydrogen. The diffusion constant was calculated in the same manner as for bulk water (see above). MSD was calculated for the atoms beginning within the Gibbs dividers, regardless of later location. Straight line fitting was performed for trajectories of ~200 ps. We propose that water is able to diffuse through a thin film of silica via hydrogen hopping, i.e., rather than diffusing as whole units, water molecules dissociate at the surface, and hydrogens diffuse through, combining with other dissociated water molecules at the other surface. This mode of diffusion has been suggested by Bakos *et al.*[52] to occur when a water molecule encounters a narrow ring. We proposed that the energy barrier for this reaction would be lower due the presence of coordination defects on the surface and within the bulk of the silica slab and could therefore be a major path of diffusion through a thin silica film containing undercoordinated silicon atoms and nonbridging oxygen (NBO) sites. Though hydrogen diffusion was observed in bulk silica, only a handful was able to cross the entire span. The diffusion constant shown here also yields estimates of the rate of this process. Order of magnitude estimates show that $\sim 10^9$ years would be required for a mole of water to diffuse through a thin (1 mm) silica container. In continuing investigations, a potential or chemical potential gradient could be used to increase this rate of crossing.

TABLE IV. Interface data. $Si(OH)_2$ is geminal silanol. Full width at half maximum is given in parentheses.

Property	Reax	Exp.
SiOH conc. (nm^{-2})	5.4	4.3–5.2,[a] 4.9[b]
$Si(OH)_2$ to SiOH ratio	0.158	0.09–0.2[a]
D_H silica bulk ($Å^2/ps$)	0.0168	···
Si coordination	3.96	···
Si–O–H bond angle	113(8.3) ± 7	···

[a]Reference 50.
[b]Reference 51.

2. Chemical properties

Since ReaxFF is able to simulate chemical reactions (the breaking and forming of bonds, which produce changes in chemical species throughout a simulation), it enables examination of the stoichiometry of the silica-water reaction. Figure 10 shows the time evolution of total number of four types of chemical species in the silica-water system. Figure 10(a) shows the total number of undercoordinated silicon atoms, while Fig. 10(b) shows the total number of NBO atoms. NBOs are defined as oxygen atoms having a bond with a silicon atom and no other bonds. Both undercoordinated silicon and oxygen atoms are clearly consumed in the reaction, approaching an equilibrium value lower than the initial value. Silanol units [Fig. 10(d)] are products of this reaction, increasing from an assumed initial value of 0. The water curve misleadingly indicates a production of water. The total number of water molecules started at 4050. The equilibrium value reached in the reaction is much lower than initial, indicating that water molecules have been consumed, despite the early transient behavior. Figure 10(c) also indicates that water dissociated within the first few picoseconds. It can be concluded that the time for the silica/water reaction to reach equilibrium is on the order of 1/2 ns.

It is clearly observed that the main product of this reaction is silanol (SiOH), in its various forms. We propose, based on Fig. 10, that reactants for this process are three-coordinated silicon atoms, one-coordinated oxygen atoms, and dissociated water. A possible equation for this reaction is

$$H_2O + 2Si + O \rightleftharpoons 2SiOH, \tag{6}$$

where Si and O are representative of undercoordinated (unfilled valency) silicon and oxygen atoms either on the silica surface or in the first few angstroms of the bulk.

Once the reaction has equilibrated, we find the equilibrium concentration of the main reactant and product, H_2O and SiOH, respectively. We find that 149 ± 2 water molecules have dissociated, while 284 ± 2 silanols have formed. Since the ratio of water dissociated to silanol formed is approximately 1:2, we propose that as each water molecule dissociates at the silica surface, the free hydrogen atom bonds to an undercoordinated oxygen on the surface, and the OH group bonds to an undercoordinated silicon atom. The equilibrium for this reaction is reached when the surface is completely hydroxylated.

3. Electrostatics

The electric dipole ($\vec{\mu}$) of water molecules in the silica-water interfacial system was computed using the same method described in Sec. III A 1. A plot of $\langle \cos(\theta) \rangle(z)$ (Fig. 11), where θ is the angle between the z-axis and $\vec{\mu}$, yields a polarized alignment of $\vec{\mu}$ with respect to the silica surface.

This alignment of charges along the silica-water interface produces a potential difference between the silica bulk and the water (taken to be ground). Charge density was calculated by dividing the system into planes along z with width of 0.5 Å and taking the sum of charges enclosed. Electric potential was calculated by integrating charge density as a function of z,[53]

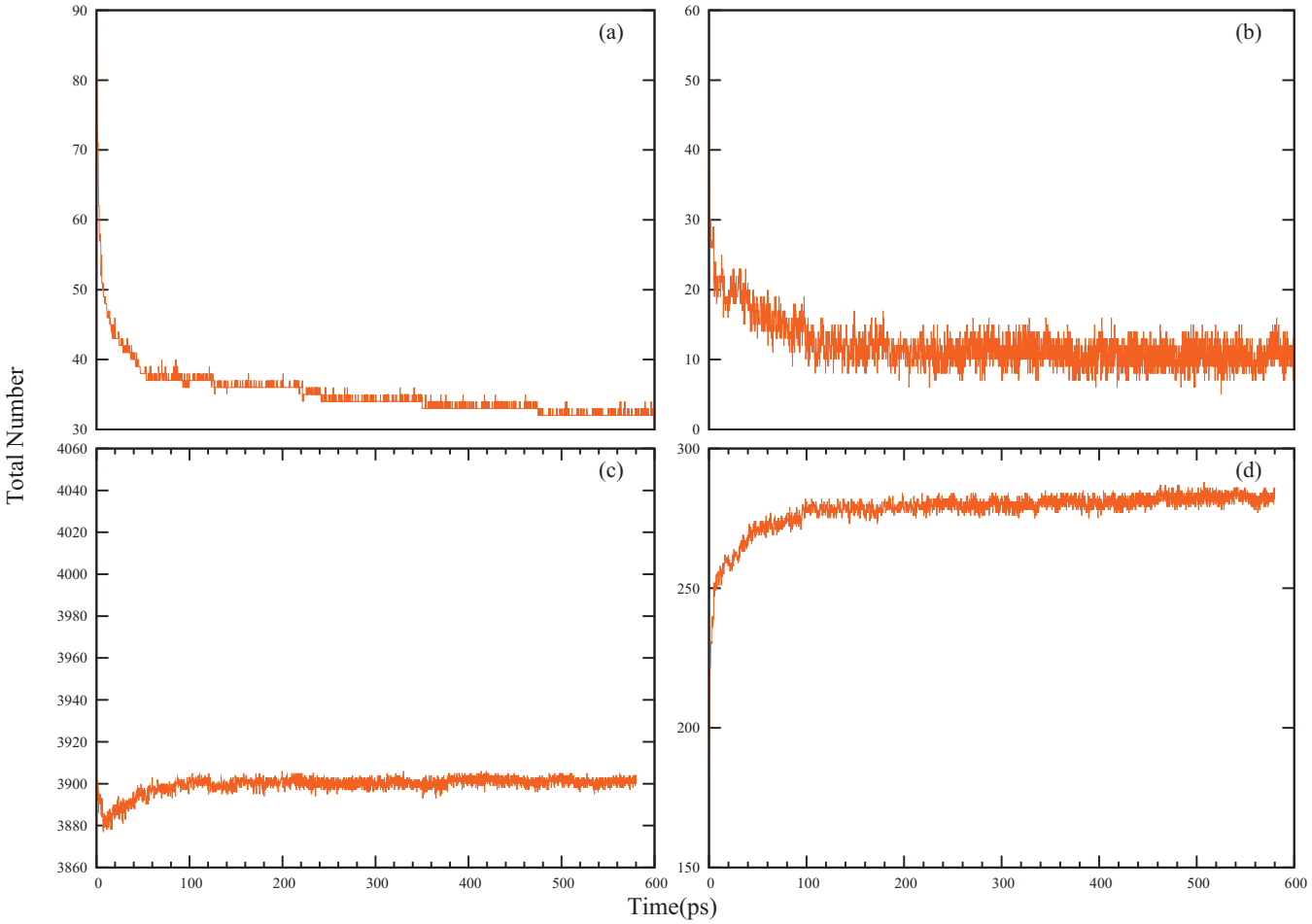

FIG. 10. Species quantities: the number of water molecules (c), silanol molecules (d), NBO atoms (b), and undercoordinated silicon atoms (a).

$$\phi(z) - \phi(z_0) = \frac{-1}{\epsilon_0} \int_{z_0}^{z} \int_{z_0}^{z'} \rho(z'') dz'' dz', \tag{7}$$

where z_0 is in the center of the bulk water, ϵ_0 is the permittivity of free space, and ρ is the charge density.

The method relies on the uniform distribution of charge within each plane along the z-axis. Since the system has periodic dimensions in x and y, each plane is mostly homogeneous. Therefore, this assumption does not introduce significant error. The system was divided in half and averaged in order to eliminate the large fluctuations in charge density that arise due to the lack of mobility in the solid silica atoms. The integrals were then performed from the outside-in (i.e., from water to the center of the silica slab) to yield the potential (Fig. 12).

Taking the water as ground, we find a potential difference of 11.5 V between the center of the silica slab to the water, with the silica at a higher potential. This large difference results from the tight alignment of water dipoles with the interface surface normal. Water molecules at the interface are nearly 75% aligned, which leads to a large charge distribution at the surface. Ong *et al.*,[54] using second harmonic generation, determined the interfacial surface potential to be higher than that of bulk water. A direct comparison between their results and values reported here is not possible due to ambiguity in identification of the interfacial surface. We also note that the potential reported here, which includes contributions from surface and dipole potentials, has the same sign and similar order of magnitude, provided the interfacial surface is appropriately chosen. Since choice of this surface is to some extent arbitrary, a quantitative comparison of these potential values is imprudent.

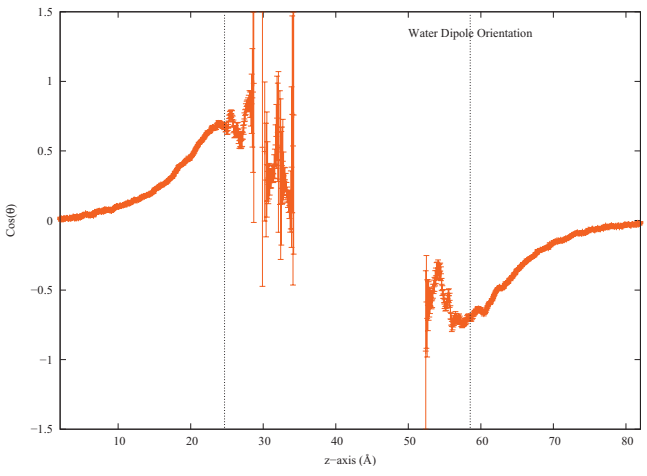

FIG. 11. Water dipole moment: orientation of water molecules given as cosine of the angle between dipole moment and surface normal (z-axis). Error bars are given as inverse square-root of number of water molecules. Gibbs dividers (dashed line) shown for reference.

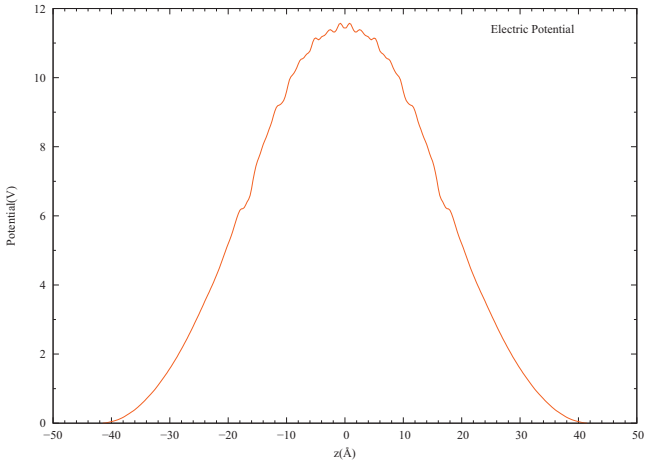

FIG. 12. Electric potential: averaged over both halves of the interface. Distance (z) shown is distance from the center of the silica slab.

IV. SUMMARY

A large silica-water interface is studied using reactive MD. This is the first simulation of its kind that achieves the length and time scales required to investigate various properties of such a system. A system of this size is necessary in order to produce a sufficient number of silanol units on the surface to allow for statistical analysis. A simulation time on the order of a half nanosecond is required to allow the system to reach equilibrium.

Our MD approach is based on a force field proposed by van Duin *et al.*[30] The specific Reax implementation (SERIALREAX) and force fields are validated by verifying structural properties of pure silica and water systems. Water properties such as bond angle and distance, charges, pair correlation data, and self-diffusion constants were used to compare with experimental and *ab initio* data. For pure silica, bond angles and distances, coordination, and pair correlations were used to validate the model.

The chemical reactions between reactive water and dangling bonds on a freshly cut silica surface are analyzed. We analyze these reactions by observing the increasing concentration of silanol units and the decreasing number of dangling bonds on the silica surface. In these simulations, reactions involving silanol groups reached chemical equilibrium in ~250 ps. It is observed that water molecules penetrate a silica film through a process similar to the Grotthuss mechanism that we call hydrogen hopping. In this process, hydrogen atoms pass through the film by associating and dissociating with oxygen atoms within the bulk silica as opposed to through diffusion of intact water molecules.

We have successfully simulated a large silica-water interface. The structural, chemical, and electrical properties of the interface are in excellent agreement with experimental and quantum chemical data available today.

ACKNOWLEDGMENTS

The authors thank Dr. David Bostick and Dr. George Khelashvili for valuable suggestions. J.CF., H.M.A., S.A.P., and A.Y.G. acknowledge the support from the Department of Energy under Grant Nos. DE-FC02-06ER25791 and DE-FC52-08NA28617. A.V.D. acknowledges support from KISK (Grant No. C000032472).

[1] M. Qhobosheane, S. Santra, P. Zhang, and W. Tan, Analyst (Cambridge, U.K.) **126**, 1274 (2001).
[2] W. Tan, K. Wang, X. He, X. Zhao, T. Drake, L. Wang, and R. Bagwe, Med. Res. Rev. **24**, 621 (2004).
[3] R. S. McDonald, J. Phys. Chem. **62**, 1168 (1958).
[4] K. Davis and M. Tomozawa, J. Non-Cryst. Solids **201**, 177 (1996).
[5] R. Sato and M. Tomozawa, J. Non-Cryst. Solids **343**, 26 (2004).
[6] R. Mozzi and B. Warren, J. Appl. Crystallogr. **2**, 164 (1969).
[7] Q. Mei, C. Benmore, S. Sen, R. Sharma, and J. Yarger, Phys. Rev. B **78**, 144204 (2008).
[8] T. Charpentier, P. Kroll, and F. Mauri, J. Phys. Chem. C **113**, 7917 (2009).
[9] A. Pedone, G. Malavasi, M. C. Menziani, U. Segre, F. Musso, M. Corno, B. Civalleri, and P. Ugliengo, Chem. Mater. **20**, 2522 (2008).
[10] C. Mischler, W. Kob, and K. Binder, Comput. Phys. Commun. **147**, 222 (2002).
[11] E. R. Cruz-Chu, A. Aksimentiev, and K. Schulten, J. Phys. Chem. B **110**, 21497 (2006).
[12] J. Du and A. N. Cormack, J. Am. Ceram. Soc. **88**, 2532 (2005).
[13] C. Wang, N. Kuzuu, and Y. Tamai, J. Non-Cryst. Solids **318**, 131 (2003).
[14] T. Mahadevan and S. Garofalini, J. Phys. Chem. C **112**, 1507 (2008).
[15] M.-H. Du, A. Kolchin, and H.-P. Cheng, J. Chem. Phys. **120**, 1044 (2004).
[16] A. A. Hassanali and S. J. Singer, J. Phys. Chem. B **111**, 11181 (2007).
[17] M. Du, A. Kolchin, and H. Cheng, J. Chem. Phys. **119**, 6418 (2003).
[18] A. C. T. van Duin, S. Dasgupta, F. Lorant, and W. A. Goddard, J. Phys. Chem. A **105**, 9396 (2001).
[19] J. Yu, S. B. Sinnott, and S. R. Phillpot, Phys. Rev. B **75**, 085311 (2007).
[20] H. M. Aktulga, S. Pandit, A. C. T. van Duin, and A. Grama, "Reactive Molecular Dynamics: Numerical Methods and Algorithmic Techniques" (submitted), available as a Purdue University Technical Report.
[21] A. K. Rappé and W. A. I. Goddard, J. Phys. Chem. **95**, 3358 (1991).
[22] Y. Saad and M. Schultz, SIAM (Soc. Ind. Appl. Math.) J. Sci. Stat. Comput. **7**, 856 (1986).
[23] K. Chenoweth, A. C. T. van Duin, and W. A. Goddard, J. Phys. Chem. A **112**, 1040 (2008).
[24] S. Nosé, J. Chem. Phys. **81**, 511 (1984).
[25] H. J. C. Berendsen, J. P. M. Postma, W. F. van Gunsteren, A. DiNola, and J. R. Haak, J. Chem. Phys. **81**, 3684 (1984)
[26] G. J. Martyna, D. J. Tobia, and M. Klein, J. Chem. Phys. **101**, 4177 (1994).
[27] K. Vollmayr, W. Kob, and K. Binder, Phys. Rev. B **54**, 15808 (1996).
[28] N. T. Huff, E. Demiralp, C. Tahir, and W. A. I. Goddard, J. Non-Cryst. Solids **253**, 133 (1999).
[29] M. Tarini, P. Cignoni, and C. Montani, IEEE Trans. Vis. Comput. Graph. **12**, 1237 (2006).
[30] A. van Duin, A. Strachan, S. Stewman, Q. Zhang, X. Xu, and W. Goddard, J. Phys. Chem. A **107**, 3803 (2003).
[31] A. C. T. van Duin, V. Bryantsev, J. Su, and W. A. Goddard, "Proton-transfer reactions" (unpublished).
[32] T. T. Trinh, A. P. J. Jansen, and R. A. van Santen, J. Phys. Chem. B **110**, 23099 (2006).
[33] H. J. C. Berendsen, J. R. Grigera, and T. P. Straatsma, J. Phys. Chem. **91**, 6269 (1987).
[34] M. Sprik, J. Hutter, and M. Parrinello, J. Chem. Phys. **105**, 1142 (1996).
[35] W. S. Benedict, N. Gailar, and E. K. Plyler, J. Chem. Phys. **24**, 1139 (1956)
[36] S. A. Clough, Y. Beers, G. P. Klein, and L. S. Rothman, J. Chem. Phys. **59**, 2254 (1973).
[37] Y. S. Badyal, M.-L. Saboungi, D. L. Price, S. D. Shastri, D. R. Haeffner, and A. K. Soper, J. Chem. Phys. **112**, 9206 (2000).
[38] R. Bentwood, A. Barnes, and W. Orville-Thomas, J. Mol. Spectrosc. **84**, 391 (1980).
[39] K. Kuchitsu and Y. Morino, Bull. Chem. Soc. Jpn. **38**, 805 (1965).
[40] A. Soper, J. Chem. Phys. **101**, 6888 (1994).
[41] K. Krynicki, C. D. Green, and D. W. Sawyer, Faraday Discuss. Chem. Soc. **66**, 199 (1978).
[42] T. A. Halgren and W. Damm, Curr. Opin. Struct. Biol. **11**, 236 (2001).
[43] D. A. Kemp and M. S. Gordon, J. Phys. Chem. A **112**, 4885 (2008).
[44] P. Chaikin and T. Lubensky, *Principles of Condensed Matter Physics*

(Cambridge University Press, Cambridge, 1995).
[45] A. Takada, P. Richet, C. Catlow, and G. Price, J. Non-Cryst. Solids **345**, 224 (2004).
[46] P. Vashishta, R. K. Kalia, and J. P. Rino, Phys. Rev. B **41**, 12197 (1990).
[47] D. I. Grimley and A. C. Wright, J. Non-Cryst. Solids **119**, 49 (1990).
[48] J. Da Silva, D. Pinatti, C. Anderson, and M. Rudee, Philos. Mag. **31**, 713 (1975).
[49] V. Sokhan and D. Tildesley, Mol. Phys. **92**, 625 (1997).
[50] E. Papirer, *Adsorption on Silica Surfaces*, Surfactant Science Series, Vol. 90 (Dekker, New York, 2000).
[51] L. Zhuravlev, Colloids Surf., A **173**, 1 (2000).
[52] T. Bakos, S. Rashkeev, and S. Pantelides, Phys. Rev. Lett. **88**, 055508 (2002).
[53] S. A. Pandit, *Soft Matter Lipid Bilayers and Red Blood Cells* (Wiley-VCH, Weinheim, 2008), Vol. 4.
[54] S. Ong, X. Zhao, and K. Eisnthal, Chem. Phys. Lett. **191**, 327 (1992).